ORIGINAL ARTICLE

Melatonin drives apoptosis in head and neck cancer by increasing mitochondrial ROS generated via reverse electron transport

Javier Florido[1,2,3]　│　Laura Martinez-Ruiz[1,2,3]　│　César Rodriguez-Santana[1,2]　│
Alba López-Rodríguez[1,2]　│　Agustín Hidalgo-Gutiérrez[1,3]　│
Cécile Cottet-Rousselle[4]　│　Frédéric Lamarche[4]　│　Uwe Schlattner[4]　│
Ana Guerra-Librero[1,2]　│　Paula Aranda-Martínez[1,2]　│
Darío Acuña-Castroviejo[1,2,3] 🔾　│　Luis C. López[1,2,3]　│　Germaine Escames[1,2,3] 🔾

[1]Institute of Biotechnology, Biomedical Research Center, Health Sciences Technology Park, University of Granada, Granada, Spain

[2]Department of Physiology, Faculty of Medicine, University of Granada, Granada, Spain

[3]Centro de Investigación Biomédica en Red Fragilidad y Envejecimiento Saludable (CIBERFES), Instituto de Investigación Biosanitaria (Ibs), Granada, San Cecilio University Hospital, Granada, Spain

[4]INSERM U1055, Laboratory of Fundamental and Applied Bioenergetics (LBFA), University of Grenoble Alpes, Grenoble, France

Correspondence
Germaine Escames, Centro de Investigación Biomédica, Parque Tecnológico de Ciencias de la Salud, Avenida del Conocimiento s/n, 18100 Armilla, Granada, Spain.
Email: gescames@ugr.es

Abstract

The oncostatic effects of melatonin correlate with increased reactive oxygen species (ROS) levels, but how melatonin induces this ROS generation is unknown. In the present study, we aimed to elucidate the two seemingly opposing actions of melatonin regarding its relationship with free radicals. We analyzed the effects of melatonin on head and neck squamous cell carcinoma cell lines (Cal-27 and SCC-9), which were treated with 0.5 or 1 mM melatonin. We further examined the potential effects of melatonin to induce ROS and apoptosis in Cal-27 xenograft mice. Here we report that melatonin mediates apoptosis in head and neck cancer by driving mitochondrial reverse electron transport (RET) to induce ROS production. Melatonin-induced changes in tumoral metabolism led to increased mitochondrial activity, which, in turn, induced ROS-dependent mitochondrial uncoupling. Interestingly, mitochondrial complex inhibitors, including rotenone, abolished the ROS elevation indicating that melatonin increased ROS generation via RET. Melatonin also increased membrane potential and $CoQ_{10}H_2/CoQ_{10}$ ratio to elevate mitochondrial ROS production, which are essential conditions for RET. We found that genetic manipulation of cancer cells with alternative oxidase, which transfers

---

Javier Florido and Laura Martinez-Ruiz authors contributed equally to this study.

2 of 15 WILEY— Journal of **Pineal Research**
Molecular, Biological, Physiological and Clinical Aspects of Melatonin

FLORIDO ET AL.

electrons from QH_2 to oxygen, inhibited melatonin-induced ROS generation, and apoptosis. RET restored the melatonin-induced oncostatic effect, highlighting the importance of RET as the site of ROS production. These results illustrate that RET and ROS production are crucial factors in melatonin's effects in cancer cells and establish the dual effect of melatonin in protecting normal cells and inducing apoptosis in cancer cells.

K E Y W O R D S
apoptosis, head and neck cancer cells, melatonin, mitochondria, oxidative damage, reactive oxygen species, reverse electron transport

1 | INTRODUCTION

Cases of cancer, which is the second-leading cause of mortality worldwide, are expected to increase by 2025,[1] and head and neck squamous cell carcinoma (HNSCC) is responsible for 500 000 new cases each year. Despite ongoing advances in surgery, radiotherapy, and chemotherapy, 5-year survival rates remain under 50%.[2,3] Recurrent HNSCC contributes to significant morbidity and portends overall poor survival,[4] and research into new therapeutic targets and treatments is quite urgent.

Because of its oncostatic influence and lack of association with adverse effects, melatonin (N-acetyl-5-methoxytryptamine) is of particular relevance to the development of innovative cancer treatments.[5–7] Several groups have reported that high concentrations of melatonin can promote reactive oxygen species (ROS) generation in a variety of cancers.[6–9]

Melatonin and its derivatives, however, are potent free radical scavengers and broad-spectrum antioxidants, which are evolutionarily conserved properties.[10,11] Thus, how ROS production is involved in melatonin's antineoplastic impact remains unclear, and elucidating this mechanism is important for possible clinical applications.

Melatonin targets mitochondria to enhance their function, maintaining mitochondrial integrity and leading to reduced electron leakage and mitochondrial ROS (mtROS) generation in nontumor cells.[1,12,13] The respiratory chain is the major source of ROS, and complexes I and III are generally regarded as the main ROS sources, whereas the contribution of intact complex II seems to be negligible.[14,15] Recent studies have highlighted an important role for reverse electron transport (RET) in producing mtROS.[15–17] RET occurs when the pool of coenzyme Q (CoQ) is over-reduced with electrons from respiratory complex II. In the presence of a high proton motive force (Δp), complex I reduces NAD^+ to NADH with electrons received from the ubiquinol pool,

generating a high level of mtROS. All of these cellular alterations may lead to apoptosis.[18]

Finally, complex I produces ROS in either the forward or reverse direction depending on the substrates used to feed the respiratory chain, suggesting that a change in cell metabolism could induce RET.[18] In this context, we have previously demonstrated that melatonin reverses metabolic reprogramming in HNSCC cells.[6] Taking these previous results together with known effects of melatonin in modifying tumor metabolism, we hypothesized that melatonin might increase mtROS by RET.

2 | MATERIALS AND METHODS

2.1 | Cell culture and treatment

The head and neck squamous carcinoma (HNSCC) cell lines Cal-27 (ATCC: CRL-2095) and SCC-9 (ATCC: CRL-1629) were obtained from the Cell Bank of the Scientific Instrumentation Centre of the University of Granada. The Cal-27 cell line was grown as previously described.[5] Previously, we performed a dose-response study, and the maximal effect was obtained at 500 and 1000 μM.[5–7] Therefore, cells were treated with melatonin 500 and 1000 μM for 48 h. The vehicle was added to the control group. Details are available in the Supporting Information.

2.2 | Measurement of ROS production and mitochondrial mass

Mitochondrial superoxide was detected using the fluorescent MitoSox Red probe and mitochondrial mass with the fluorescent MitoTracker Green probe.

ROS production was measured using 2′,7′-dichlorofluorescein diacetate (DCFH-DA) as previously described.[6] Details are available in the Supporting Information.

2.3 | Apoptosis

Apoptotic cells were detected using an annexin V/propidium iodide (PI) kit (ANXVKF-100T; Inmunostep). Once cells were treated as described above, annexin V/PI staining was performed according to the manufacturer's instructions. HNSCC cells were analyzed using a flow cytometer (Becton Dickinson FACSCanto II cytometer).

2.4 | Calcium retention capacity in digitonin-permeabilized cells

The calcium retention capacity was measured in digitonin-permeabilized cells by adding sequential Ca^{2+} pulses until mitochondrial permeability transition pore (mPTP) was opened. Measurements of extramitochondrial Ca^{2+} were carried out fluorometrically.[19,20] Details are available in the Supporting Information.

2.5 | Western blot analysis

Protein extraction and western blot analyses were performed as previously described[6] and the Bradford assay was used to determine protein concentration. Details are available in the Supporting Information.

2.6 | Electron transport chain (ETC) complex activity assays

Mitochondrial respiratory chain activities were measured for each complex using kits from Abcam according to the manufacturer's instructions. Details are available in the Supporting Information.

2.7 | Measurement of mitochondrial respiration

Oxygen consumption rate (OCR) was determined using the Seahorse Extracellular Flux (XF-24) analyzer as previously described.[6] Details are available in the Supporting Information.

2.8 | Measurement of oxygen consumption in intact cells

Oxygen consumption was measured into a thermostatically controlled oxygraph vessel equipped with a Clark oxygen electrode at 37°C (Strathkelvin MS200A system).[21] Details are available in the Supporting Information.

2.9 | Measurement of oxygen consumption in digitonin-permeabilized cells

Oxygen consumption was measured in digitonin-permeabilized cells in a thermostatically controlled oxygraph vessel equipped with a Clark oxygen electrode at 37°C.[21] Details are available in the Supporting Information.

2.10 | Determination of adenosine triphosphate (ATP) levels

ATP concentration was determined using the ATP assay kit from Abcam according to the manufacturer's instructions. Details are available in the Supporting Information.

2.11 | Determination of CoQ_{10} and $CoQ_{10}H_2$ by liquid chromatography and mass spectrometry (UPLC-MS/MS)

CoQ_{10} pools were extracted as previously described[22] and analyzed by ultraperformance liquid chromatography (UPLC) with tandem mass spectrometry (MS/MS). The UHPLC system was coupled online with a Q Exactive Focus mass spectrometer (Thermo) as previously described.[23] Data were analyzed using Tracefinder 4.1 software (Thermo). Details are available in the Supporting Information.

2.12 | Mitochondrial membrane potential analysis

Mitochondrial membrane potential was measured by fluorometric analysis using tetramethylrhodamine ethyl ester (TMRE) with the microplate fluorescence reader FL × 800 (Bio-Tek Instruments) at 549 nm to excitation and 575 nm to emission.[24] Details are available in the Supporting Information.

2.13 | Mitochondrial mass analysis by flow cytometry

Cell suspensions were incubated in the presence of 50 nM of Mitotracker GreenFM for mitochondrial mass measurement for 15 min in a 5% CO_2 humidified

atmosphere at 37°C and protected from light. They then were immediately analyzed by fluorescence-activated cell sorting at 488 nm to excitation and 530 nm to emission.[25]

2.14 | Determination of tricarboxylic acid (TCA) cycle intermediates by UPLC-MS/MS

TCA intermediates were extracted as previously described.[26] Samples were then analyzed by UPLC-MS/MS. Data were acquired with MassLynx 4.0 software and calibrated and quantified by QuanLynx software. Details are available in the Supporting Information.

2.15 | NAD/NADH quantification

NAD+ levels were measured using a oxidized and reduced nicotinamide adenine dinucleotide (NAD/NADH) assay kit (ab65348; Abcam) according to the manufacturer's instructions. NAD+ and NADH levels were measured with a microplate reader spectrophotometer (Power Wave X-1) at 450 nm. Values for NAD+ and NADH levels were determined from a standard calibration curve. NAD+ and NADH concentrations were normalized by protein content as measured using the Bradford assay.

2.16 | Evaluation of supercomplex (SC) formation by blue native gel electrophoresis (BNGE)

BNGE was performed on crude mitochondrial fractions as previously described.[27] Details are available in the Supporting Information.

2.17 | Production of alternative oxidase (AOX) stable lines

Lentiviral vectors carrying the cDNA encoding an AOX (sequence from *Ciona intestinalis* genome, DM193474.1, 1110 pb) were used to generate a Cal-27 cell line expressing AOX. The AOX stable cell line was established according to the manufacturer's instructions. Details are available in the Supporting Information.

2.18 | Animal models

All animal experiments were performed following a protocol approved by the Institutional Animal Care and Use Committee of the University of Granada (procedures 11-CEEA-OH-2013), developed in accordance with the European Convention for the Protection of Vertebrate Animals used for Experimental and Other Scientific Purposes (CETS # 123) and Spanish law (R.D. 53/2013). Details are available in Supporting Information.

2.19 | Histology

Apoptosis was evaluated using the DeadEnd Fluorometric terminal deoxynucleotidyl transferase dUTP nick end labeling (TUNEL) (G3250; Promega) system in tumor tissue sections following the manufacturer's indications. Hoechst (33342; ThermoFisher Scientific) was used to stain the nuclei. Images were acquired under fluorescence microscopy (Nikon Eclipse Ni-U microscope), with quantification of TUNEL+ per field using five random fields per slide. Images were analyzed with ImageJ software. Details are available in Supporting Information.

2.20 | Data and statistical analysis

All statistical analyses were performed using Prism 8 scientific software (GraphPad Software Inc.). Unpaired Student's *t*-tests were used to compare differences between experimental groups and their respective untreated controls. Data were expressed as the mean ± standard error of the mean of a minimum of three independent experiments. A $p < .05$ was considered statistically significant.

3 | RESULTS

3.1 | Melatonin induces apoptosis via ROS-dependent production

As the direct anticancer effects of melatonin correlate with increased ROS levels and increased apoptosis in HNSCC,[6] we first analyzed ROS levels by MitoSox-Red and MitoTracker green fluorescent staining (Figure 1A) and fluorometric techniques (Figure 1B). Consistent with previous findings,[5–7] melatonin treatment induced an increase in ROS production in Cal-27 cells, especially after 48 h at 500 or 1000 μM (Figure 1A,B), which correlated with a marked increase in apoptosis (Figure 1C). Similar results were obtained in SCC-9 cells (Supporting Information: Figure S1A,B). Of note, pretreating cancer cells with N-acetylcysteine (NAC) at 5 mM to scavenge ROS (Figure 1D) inhibited melatonin-induced apoptosis (Figure 1E).
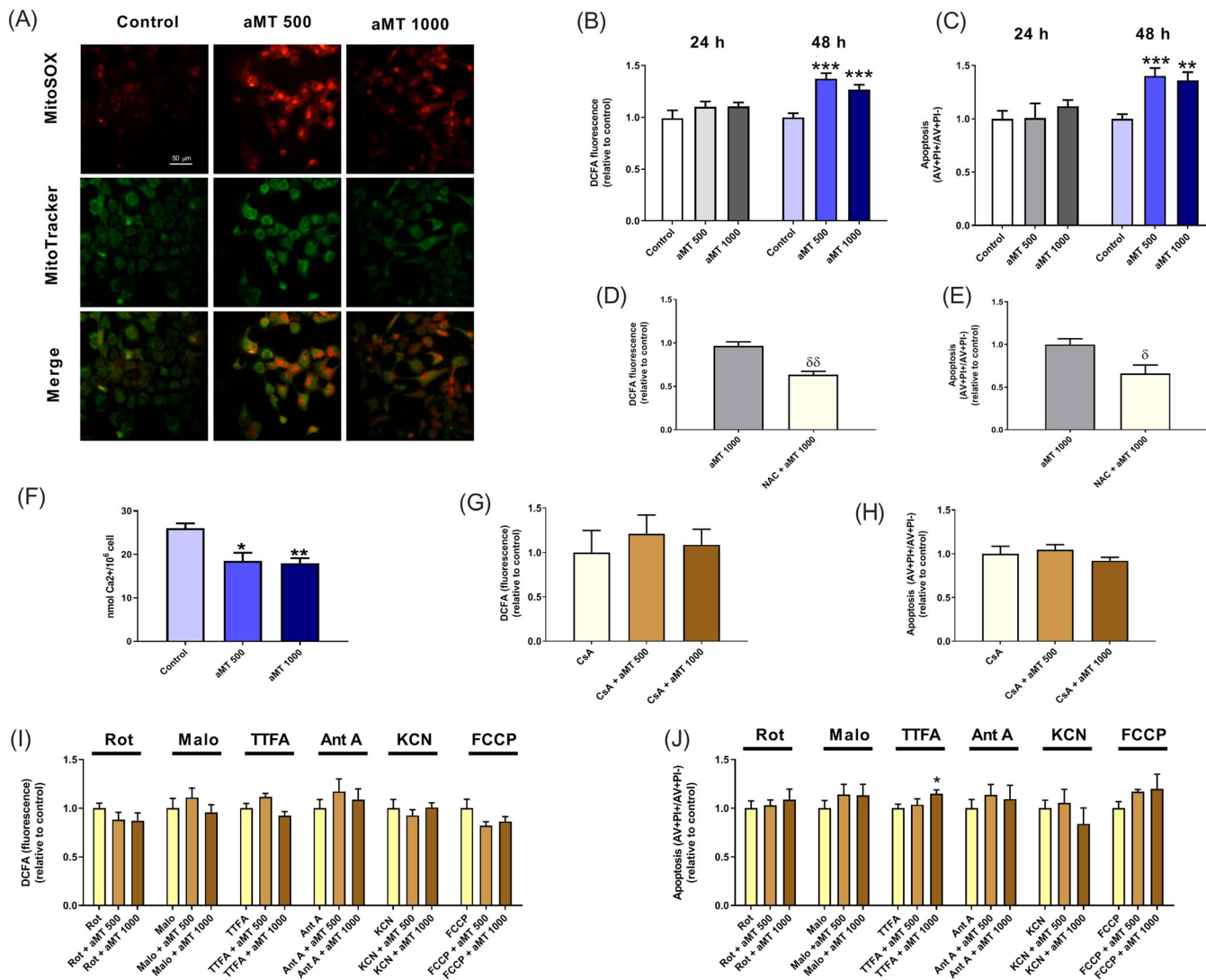
FIGURE 1 mtROS production drives melatonin-induced proapoptotic effects in Cal-27. (A) ROS (red) and mitochondria (green) detected by fluorescence microscopy after incubation with MitoSox-Red (5 μM) and MitoTracker (50 nM) for 20 min in Cal-27 cells treated with melatonin (aMT) for 48 h. Scale bar = 50 μm. (B) Measurements of intracellular ROS levels by fluorimetry after staining with the DCFA fluorescent probe after 24 and 48 h of melatonin treatment. (C) Apoptosis level (AV+/PI+ and AV+/PI−) analyzed by flow cytometry after 24 and 48 h of melatonin treatment. For (A–C), treatment groups included vehicle (control) and melatonin (aMT) at a concentration of 500 or 1000 μM for 24 h (gray range) or 48 h (blue range) in Cal-27 cells. (D) Measurements of intracellular ROS levels by fluorimetry after staining with the DCF fluorescent probe in Cal-27 cells treated with melatonin at 1000 μM alone and pretreated with NAC 5 mM. (E) Apoptosis level (AV+/PI+ and AV+/PI−) analyzed by flow cytometry in Cal-27 cells treated with melatonin at 1000 μM alone and pretreated with NAC 5 mM. (F) Calcium retention capacity detected by fluorometric assay in Cal-27 cells treated with melatonin at 500 or 1000 μM for 48 h. (G) Measurements of intracellular ROS levels by fluorimetry after staining with the DCF fluorescent probe in Cal-27 cells treated with melatonin at 500 or 1000 μM for 48 h and pretreated with CsA at 1 μM. (H) Apoptosis level (AV+/PI+and AV+/PI−) analyzed by flow cytometry in Cal-27 cells treated with melatonin at 500 or 1000 μM for 48 h and pretreated with CsA at 1 μM. (I) Measurements of intracellular ROS levels by fluorimetry after staining with the DCF fluorescent probe in Cal-27 cells treated with melatonin at 500 or 1000 μM for 48 h and pretreated with 3 nM rotenone, 10 mM malonate, 50 μM TTFA, 2 μM ant A, 200 μM KCN, or 200 nM FCCP. (J) Apoptosis level (AV+/PI+ and AV+/PI−) analyzed by flow cytometry in Cal-27 cells treated with melatonin at 500 or 1000 μM for 48 h and pretreated with 3 nM rotenone, 10 mM malonate, 50 μM TTFA, 2 μM antimycin A, 200 μM KCN, or 200 nM FCCP. Data are presented as mean ± standard error of the mean (n = 4–10 for each group; one-tailed unpaired t-test; *$p < .05$; **$p < .01$; ***$p < .001$ vs. control; $^\delta p < .05$, $^{\delta\delta}p < .01$ vs. aMT 1000 μM). ant A, antimycin A; AV, annexin V; DCF, 2′,7′-Dichlorodihydrofluorescein; DCFA, dichlorodihydrofluorescein diacetate; FCCP, carbonylcyanide-p-trifluoromethoxyphenylhydrazone; KCN, potassium cyanide; mtROS, mitochondrial ROS; NAC, N-acetylcysteine; PI, propidium iodide; ROS, reactive oxygen species; TTFA, thenoyltrifluoroacetone

ROS production may trigger mPTP with further stimulation of ROS. Therefore, we measured the calcium retention capacity in Cal-27 cells treated with melatonin at 500 or 1000 μM after 48 h. Melatonin treatment decreased calcium retention capacity for both cell lines (Figure 1F and Supporting Information: Figure S1C), indicating that it increased the mPTP opening state in Cal-27 and SCC-9 cells. To corroborate whether the mPTP opening state induced apoptosis, cells were pretreated with an mPTP opening inhibitor, cyclosporin A (CsA) at 1 μM in both cell lines. As shown in Figure 1G and Supporting Information: Figure S1D, CsA decreased melatonin-induced ROS production. Moreover, consistent with the above results, the reduced ROS production led to decreased apoptosis (Figure 1H and Supporting Information: Figure S1E). Overall, these findings suggest that the apoptotic effect of melatonin arises from ROS-induced mPTP opening. These data further support that melatonin-induced apoptosis requires sustained ROS production.

To investigate whether the activity of ETC complexes is essential for ROS production, we applied different inhibitors of mitochondrial respiration. Of interest, pretreatment of Cal-27 and SCC-9 cells with rotenone, malonate, thenoyltrifluoroacetone, antimycin A, potassium cyanide, or carbonylcyanide-p-trifluoromethoxyphenylhydrazone (FCCP) inhibited melatonin-induced ROS production (Figure 1I and Supporting Information: Figure S1F). As expected, these results correlated with decreased melatonin-induced apoptosis (Figure 1J and Supporting Information: Figure S1G). These findings suggest that melatonin acts through high mitochondrial complex activities and high membrane potential to elevate mitochondrial ROS production and that all mitochondrial complex inhibitors, including rotenone, can abolish the ROS elevation (Figure 1I and Supporting Information: Figure S1F). Rotenone inhibits complex I RET,[18,28] so it is possible that melatonin alters mitochondrial respiration via RET.

3.2 | Melatonin induces mitochondrial uncoupling in HNSCC cells

Mitochondrial ROS burst is a hallmark of complex I RET, and the activity of ETC complexes and the mitochondrial proton gradient is essential for RET.[15] For these reasons, to elucidate the mechanism underlying the melatonin-induced ROS increase, we analyzed mitochondrial function in HNSCC cells. We evaluated OXPHOS protein levels by western blot analysis and OXPHOS activity by spectrophotometric analysis (Figure 2A–K). In agreement with the effects of melatonin in nontumor tissues,[12,29–31] melatonin increased the levels of complexes I and IV relative to control

cells at 1000 μM after 48 h of treatment (Figure 2A,D). This increase was reflected primarily in increased complex I and IV activities after 24 h of treatment (Figure 2G,J). To our surprise and in contrast to results with the mitochondria of nontumor cells,[30] melatonin at 48 h highly increased levels of complex II, and at 24 h increased its activity, at 1000 μM (Figure 2B,H). Complex III and complex V were unaffected (Figure 2C,E,I,K). Furthermore, we found a decrease in complex II and complex V activity after 48h of melatonin treatment at 1000 μM (Figure 2H,K), suggesting that the high concentration of melatonin during longer treatments decreased mitochondrial function.

Next, using the Seahorse XF24 extracellular flux analyzer, we examined whether the change in mitochondrial complexes correlated with increased mitochondrial respiration. Again, to our surprise and in contrast to results observed for complex activities, melatonin did not modify the OCR corresponding to basal respiration (Figure 2L,M). However, melatonin induced increased electron transport system (ETS) within 24 h in Cal-27 cells treated with 1000 μM melatonin, without any change at 48 h (Figure 2L,N). These results were confirmed using an oxygraph vessel equipped with a Clark oxygen electrode (Supporting Information: Figure S2A,B), indicating that melatonin treatment did not modify basal OCR after 48 h of treatment.

To further confirm these results, we conducted experiments using oxygraph respiration in permeabilized Cal-27 cells. OCR was measured in the presence of glutamate/malate (G/M) (Figure 2O) or succinate as substrates (state 2) (Figure 2P), after the addition of adenosine diphosphate (state 3) and followed by the addition of oligomycin (state 4). Consistent with the results obtained with intact cells (Supporting Information: Figure S2A), melatonin at any dose did not modify the respiratory control ratio (RCR: state 3/state 4) with G/M, related to complex I-dependent respiration (Figure 2O). However, melatonin decreased the RCR with succinate, which is related to complex II-dependent respiration (Figure 2P). These data suggest that melatonin induced an increase in some components of the ETC (complexes I, II, and IV) without increasing mitochondrial respiration, suggesting uncoupling between the ETC and phosphorylation in the mitochondria of Cal-27 cells.

To clarify the partial uncoupling between respiration and oxidative phosphorylation in mitochondria induced by melatonin, we analyzed steady-state levels of ATP by fluorometric assay (Figure 2Q) and adenosine monophosphate-activated protein kinase (AMPK) activation, which depends on the AMP/ATP ratio, by western blot analysis (Figure 2R,S). Melatonin reduced ATP levels after 48 h of treatment and activated AMPK (Figure 2Q–S), confirming that melatonin induced a mitochondrial uncoupling in Cal-27 cells, increasing mtROS production.
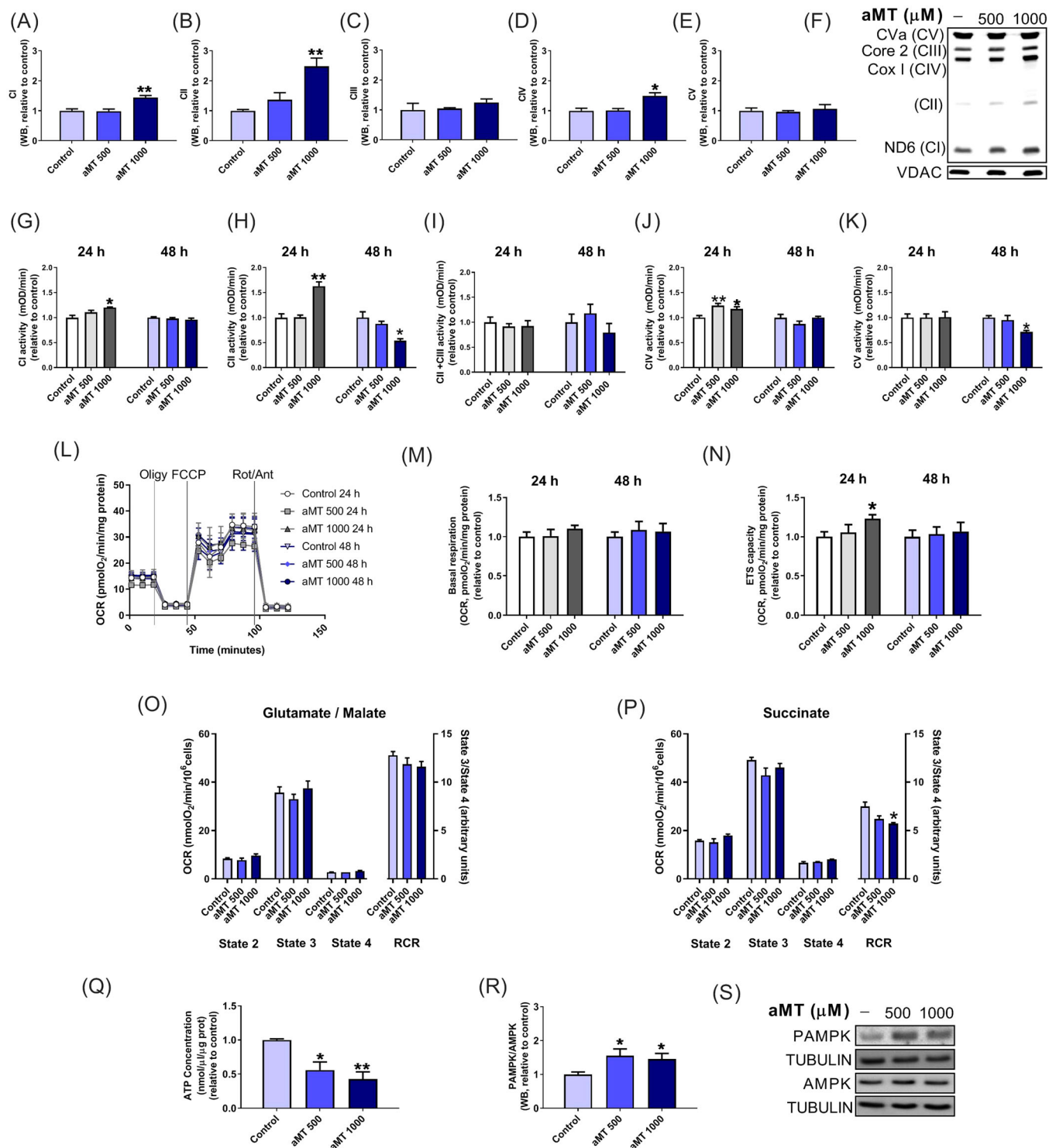
FIGURE 2 Effect of melatonin on mitochondrial function in the HNSCC Cal-27 cell line. (A–F) Analysis of OXPHOS protein expression by western blot (WB). (G–K) Analysis of mitochondria complex (CI–CV) activity by spectrophotometric analysis. (L–N) OCR corresponding to (M) basal respiration and (N) ETS capacity, as analyzed by SeaHorse. (O) OCR in digitonin-permeabilized Cal-27 cells with glutamate/malate without ADP (state 2), in the presence of 500 μM ADP (state 3) or 0.16 μg/ml oligomycin A (state 4), and RCR calculation (state 3/state 4). (P) OCR in digitonin-permeabilized Cal-27 cells with succinate without ADP (state 2), in the presence of 500 μM ADP (state 3) or 0.16 μg/ml oligomycin A (state 4), and RCR calculation (state 3/state 4). (Q) Ratio of ATP levels measured by fluorometric test. (R,S) Ratio of PAMPK and AMPK expression analyzed by western blot. Treatment groups included vehicle (control) and melatonin (aMT) at 500 or 1000 μM for 24 h (gray range) or 48 h (blue range) in Cal-27 cells. Data are presented as mean ± standard error of the mean (n = 3–8 for each group; one-tailed unpaired t-test; *$p < .05$; **$p < .01$ vs. control). ADP, adenosine diphosphate; ETS, electron transport system; HNSCC, head and neck squamous cell carcinoma; OCR, oxygen consumption rate; OD, optical density; AMPK, adenosine monophosphate protein kinase; PAMPK, phosphorylated adenosine monophosphate protein kinase; RCR, respiratory control ratio; WB, western blot
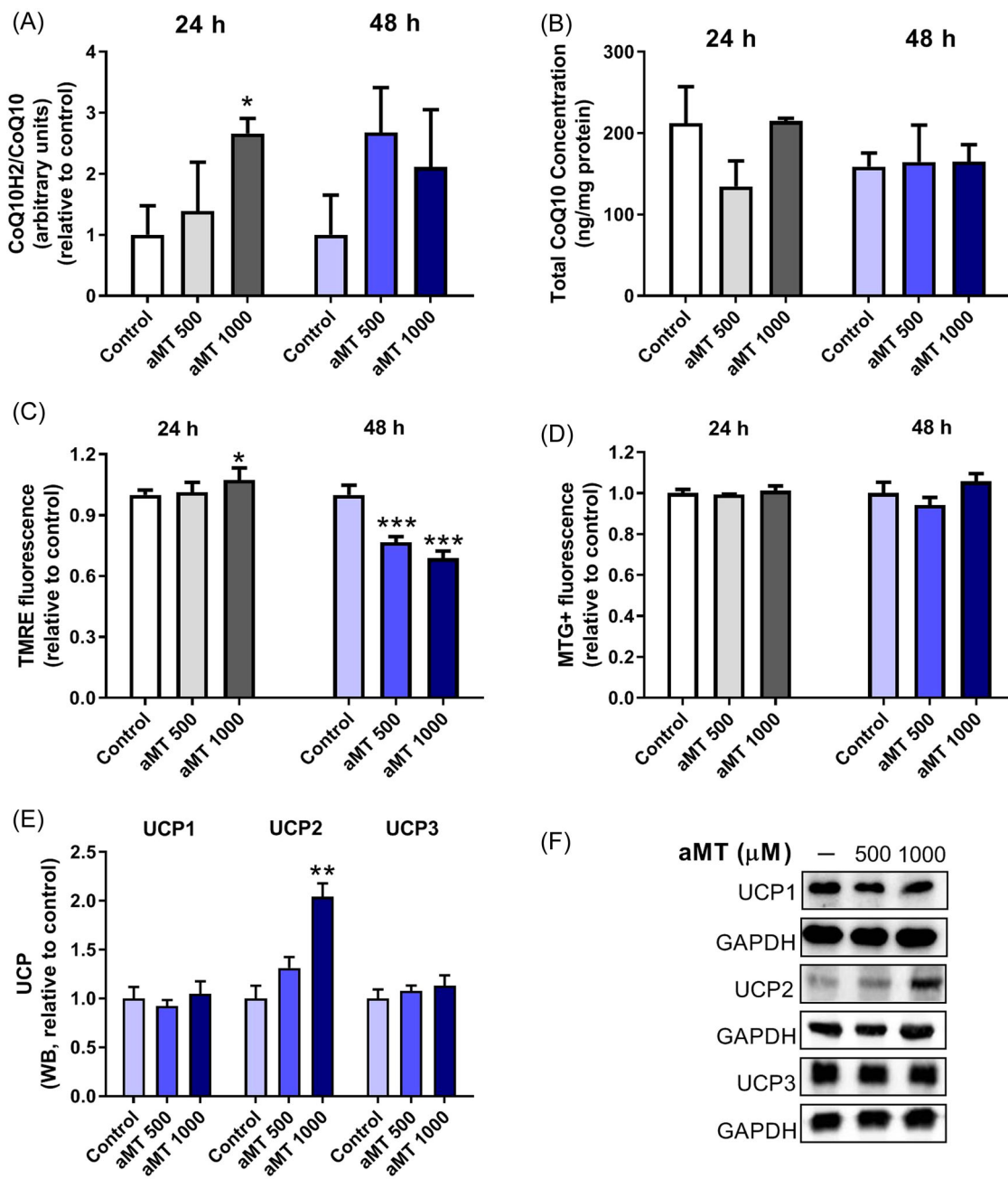
8 of 15 | WILEY | *Journal of* **Pineal Research**
Molecular, Biological, Physiological and
Clinical Aspects of Melatonin

FLORIDO ET AL.

FIGURE 3 Increased RET-ROS by modification of CoQ redox and mitochondrial membrane potential in Cal-27 cells treated with melatonin. (A, B) CoQ10 and CoQ10H$_2$/CoQ10 ratio analyzed by UPLC-MS/MS. (C, D) (C) Mitochondrial membrane potential and (D) mitochondrial mass analyses by fluorimetry after staining with TMRE or MTG fluorescent probe, respectively. (E, F) Western blot analysis of UCP-1, UCP-2, and UCP-3. Treatment groups included vehicle (control) and melatonin (aMT) at 500 or 1000 μM for 24 h (gray range) or 48 h (blue range) in Cal-27 cells. Data are presented as mean ± standard error of the mean (n = 3–8 for each group; one-tailed unpaired t-test; *$p < .05$; **$p < .01$; ***$p < .001$ vs. control). CoQ, coenzyme Q; MS, mass spectrometry; MTG, mitotracker green; RET, reverse electron transport; ROS, reactive oxygen species; TMRE, tetramethylrhodamine ethyl ester; UCP, uncoupling protein; UPLC, ultraperformance liquid chromatography.

3.3 | Melatonin increases RET-ROS by modification of the CoQ redox state and mitochondrial membrane potential (Δψm)

Given that RET occurs when the pool of CoQ is over-reduced with electrons from respiratory complex II[17,32]

and that melatonin notably increased complex II activity and expression (Figure 2B,H), we analyzed the CoQ redox state by UPLC-MS/MS (Figure 3A,B). Consistent with our prediction, melatonin 1000 μM enhanced the CoQ$_{10}$H$_2$/CoQ$_{10}$ ratio after 24 h of treatment (Figure 3A), without increasing total CoQ (Figure 3B). We obtained

similar results with melatonin after 48 h of treatment (Figure 3A,B).

The production of mitochondrial ROS via complex I RET tightly depends on high $\Delta\psi m$, and even a slight decrease in $\Delta\psi m$ induced by FCCP reduces ROS generation via complex I RET.[33] As we showed above, pretreatment of Cal-27 cells with FCCP abolished the melatonin-induced mitochondrial ROS burst (Figure 1I). Moreover, cell incubation with melatonin for 24 h significantly increased $\Delta\psi m$ in Cal-27 cells (Figure 3C) without altering the mitochondrial mass, as measured by MitoTracker Green FM fluorescence (Figure 3D), further supporting melatonin-induced ROS generation via complex I RET. However, we observed a drop in $\Delta\psi m$ after 48 h of melatonin treatment (Figure 3C), which could be explained by the fact that melatonin-induced sustained ROS production after 48 h may trigger mPTP opening (Figure 1F), inducing $\Delta\psi m$ decline. Because uncoupling proteins (UCPs) are the direct downstream mediators of ROS-dependent mitochondrial production[34] related to a drop in $\Delta\psi m$, we analyzed UCP protein levels by western blot analysis. As shown in Figure 3F,E, melatonin significantly increased UCP2 levels in a dose-dependent manner, explaining the steep reduction in $\Delta\psi m$.

3.4 | Melatonin increases RET-ROS by modification of metabolism

To examine how melatonin induces a modification of metabolism, we first carried out metabolomic analyses using UPLC-MS/MS and found that melatonin upregulated key TCA cycle metabolites in Cal-27 cells (Figure 4A–D), especially succinic acid, the principal substrate of RET (Figure 4A). This upregulation led to an increased NADH/NAD ratio (Figure 4E), further supporting that melatonin induced ROS generation via complex I RET.

When fatty acids are oxidized, NADH increases, resulting in an over-reduction of the CoQ pool and an increase in RET-ROS.[35] We analyzed medium-chain acyl-CoA dehydrogenase (MCAD) and enoyl-CoA hydratase and 3-hydroxyacyl CoA dehydrogenase (EHHADH), which regulate fatty acid oxidation, and acetyl-CoA carboxylase (ACC), which is involved in lipid biosynthesis.[36] In a dose- and time-dependent manner, melatonin triggered increased levels of medium-chain acyl-CoA dehydrogenase (Figure 4F,I), with a tendency for EHHADH at 48 h (Figure 4G,I), and an increased phosphorylated/No- phosphorylated acetyl-CoA carboxylase ratio (Figure 4H,I), most likely

due to the activated phosphorylated adenosine monophosphate protein kinase. Collectively, these results suggest that melatonin activated fatty acid oxidation as well as inhibiting lipid biosynthesis.

The high $CoQ_{10}H_2/CoQ_{10}$ ratio during β-oxidation leads to RET-produced ROS and localized RET leads to changes in SC formation.[35] As expected, melatonin reduced the formation of SCs involving complex I (Figure 4J,M) but increased the formation of SCs involving complex III within 48 h in a dose-dependent manner (Figure 4K–M). These results indicate that melatonin rearranges the formation of SCs degrading CI and stimulating the formation of complexes III + IV SCs to favor the oxidation of fatty acids. These findings support the important role of melatonin in inducing changes in HNSCC cell metabolism, indicating that melatonin could be exerting its oncostatic effect via RET-ROS.

3.5 | AOX expression reduces RET and inhibits melatonin's oncostatic effects in vitro and in vivo

To confirm whether RET underlies melatonin-induced ROS production in HNSCC cells, we used the AOX, a cyanide-insensitive oxidase that transfers electrons from QH_2 to oxygen, decreasing the $CoQH_2/CoQ$ ratio.[16] For this reason, we expressed AOX in Cal-27 cells to examine whether reducing $CoQ_{10}H_2$ accumulation decreased ROS production and then apoptosis. AOX expression restored a normal $CoQ_{10}H_2/CoQ_{10}$ ratio (Figure 5B) without inducing significant changes in the total CoQ_{10} amount (Figure 5A). Moreover, the effects of melatonin in inducing ROS production and apoptosis were abolished in cells expressing AOX (Figure 5C,D). This result indicated that complex I RET induced by melatonin is also required for melatonin-induced sustained ROS production. Furthermore, to ensure AOX functionality, cells were treated with complex III inhibitor antimycin A. AOX cell line showed an increase in Cal-27 cell proliferation and mitochondrial respiration compared to WT in presence of antimycin A, indicating AOX functionality (Supporting Information: Figure S5).

We further confirmed these results in vivo, using mice injected with wild-type Cal-27 cells or cells expressing AOX. Considering that our in vivo previous results suggested that melatonin administered intraperitoneally did not reach the mitochondria at a sufficient concentration,[5] both groups were treated intratumorally with vehicle or with melatonin, which did not reach the plasma increasing melatonin
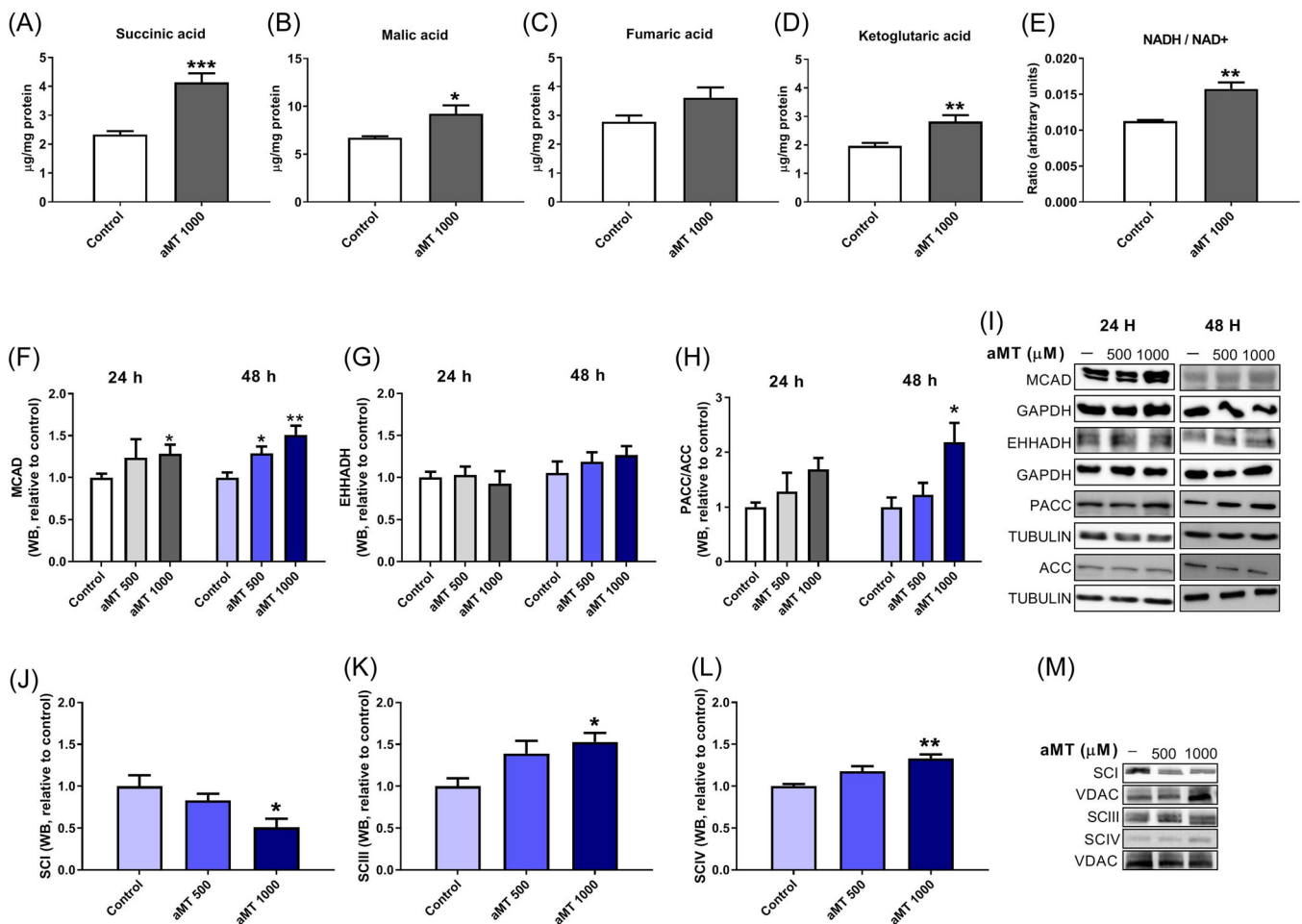
FIGURE 4 Melatonin-induced change in Cal-27 cell metabolism by upregulation of fatty acid oxidation and TCA metabolites. (A–D) Metabolomic study of intracellular levels of (A) succinic acid, (B) fumaric acid, (C) malic acid, and (D) ketoglutaric acid. (E) NADH and NAD+ levels measured using a colorimetric test and expressed as a ratio. (F–I) Western blot analysis of (F) MDAC, (G) EHHADH, and (H) PACC/ACC ratio. (J–M) Evaluation of SC formation by BNGE. Treatment groups included vehicle (control) and melatonin (aMT) at 500 or 1000 μM for 24 h (gray range) or 48 h (blue range) in Cal-27 cells. Data are presented as mean ± standard error of the mean ($n = 3$–7 for each group; one-tailed unpaired t-test; *$p < .05$; **$p < .01$; ***$p < .001$ vs. control). BNGE, blue native gel electrophoresis; EHHADH, enoyl-CoA hydratase and 3-hydroxyacyl CoA dehydrogenase; PACC/ACC, phosphorylated/no- phosphorylated acetyl-CoA carboxylase; SC, supercomplex; TCA, tricarboxylic acid.

level into the tumor. After 35 days of treatment, melatonin, which reduced greatly the tumor volume in wild-type Cal-27 cells, did not have any effect on volume in tumors containing cells expressing AOX (aMT 3% AOX) compared with its controls (Figure 5E). To investigate whether melatonin-induced complex I RET led to apoptosis, we analyzed carbonyl protein level and apoptosis using the TUNEL assay. As shown in Figure 5F–H, the effects of melatonin in increasing ROS production and apoptosis disappeared in tumors expressing AOX (aMT AOX) compared with controls. Overall, these findings support that melatonin induces ROS generation via complex I RET.

4 | DISCUSSION

Melatonin has two seemingly opposing actions regarding its relationship with free radicals. Numerous studies have shown that it plays an effective role in maintaining mitochondrial homeostasis,[12,29–31,37] but the mechanism by which melatonin induces ROS production in cancer cells is poorly understood. In this study, we provided evidence that melatonin mediates apoptosis in HNSCC cells by targeting mitochondria to induce ROS by complex I RET.

The complex role of ROS in mediating tumor progression remains a subject of controversy. Cancer cells often exhibit altered mitochondrial function,
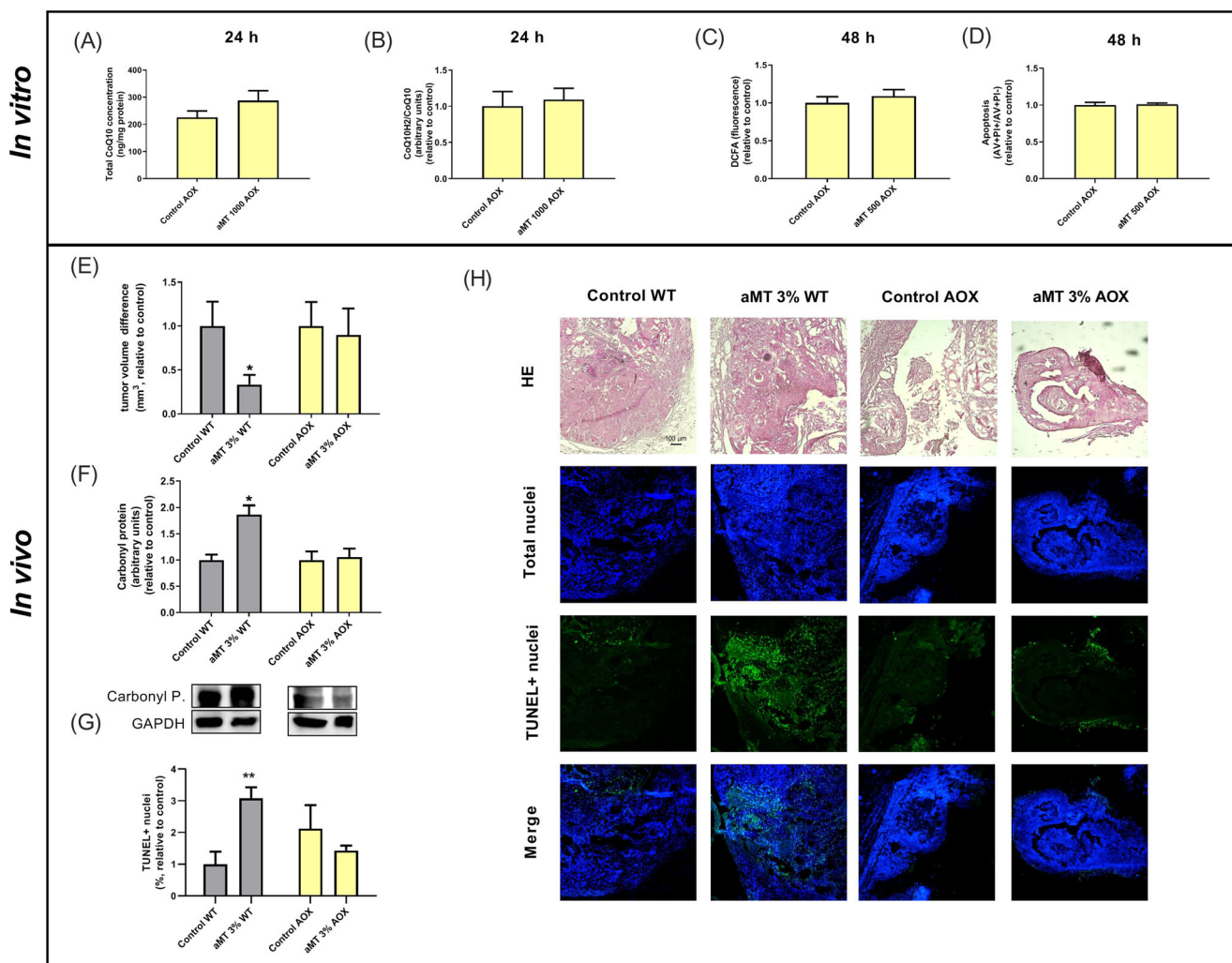
FIGURE 5 Melatonin-induced oncostatic effects are inhibited in Cal-27 expressing AOX in vitro and in vivo. (A,B) (A) Levels of total CoQ10 and (B) CoQ10H2/CoQ10 ratio in Cal-27 cells expressing AOX in vitro, analyzed by UPLC-MS/MS. Groups included vehicle (control) and melatonin (aMT) at 1000 μM for 24 h (treatment with the greatest difference vs. wild-type Cal-27). (C) Measurements in vitro of intracellular ROS levels by fluorimetry after staining with the DCF fluorescent probe in Cal-27 cells expressing AOX. Groups included vehicle (control) and melatonin (aMT) at 500 μM for 48 h (treatment with the greatest difference vs. wild-type Cal-27). (D) Apoptosis level (AV+/PI+ and AV+/PI−) analyzed in vitro by flow cytometry in Cal-27 cells expressing AOX. Groups included vehicle (control) and melatonin (aMT) at 500 μM for 48 h (treatment with the greatest difference vs. wild-type Cal-27). (E) Tumor volume difference analyzed in vivo with a caliper vernier. (F) Western blot analysis of carbonyl protein. (G,H) (H) TUNEL+ nuclei (apoptotic nuclei, green) and DAPI-stained nuclei (total nuclei, blue). Scale bar = 100 μm. (G) The percentage of apoptotic cells was designated as the apoptotic index. For (E–G), treatment groups included WT Cal-27 xenograft treated intratumorally with vehicle (control WT) and melatonin at 3% (aMT 3% WT) or Cal-27–expressing AOX xenograft treated intratumorally with vehicle (control AOX) and melatonin at 3% (aMT 3% AOX). Data are presented as mean ± standard error of the mean ($n = 3$–8 for each group; one-tailed unpaired t-test; *$p < .05$; **$p < .01$ vs. control). AOX, alternative oxidase; CoQ, coenzyme Q; DAPI, 4′,6-diamidino-2-phenylindole; DCF, 2′,7′-dichlorodihydrofluorescein; TUNEL, terminal deoxynucleotidyl transferase dUTP nick end labeling; WT, wild type.

including elevated ROS generation,[38,39] which is involved in the initiation and progression of cancer.[40,41] However, toxic levels of ROS production in cancers are antitumorigenic.[5–7,42] The current findings show that melatonin-induced apoptosis was abolished by pretreatment of Cal-27 cells with the antioxidant NAC, suggesting that ROS levels are increased by melatonin above a toxicity threshold that results in oxidative damage and cell death.

Moreover, an amplified ROS signal may cause perceptible mitochondrial and cellular injury.[43] It seems that the main sites of mtROS generation in vivo are respiratory complexes I and III.[18,28] However, under specific conditions such as hypoxia, complex II subunits can lead to increased ROS generation via RET.[18,28] One way to differentiate RET-ROS production is by using rotenone, which increases ROS production in the

forward direction, but decreases it via RET.[44] Our current findings indicate that ROS production induced by melatonin was reduced under complex I inhibition with rotenone. Moreover, melatonin increased the expression and activities of complexes I, II, and IV, as well as ETS capacity, and especially surprising to us was the significant increase in complex II with no effect on complex III. Complex II can adapt to different roles as a producer or modulator of mtROS depending on the activity of other complexes such as complex III.[15] In contrast, we observed a lack of effect of melatonin on complex V with a decrease in ATP production, which, in part, supports an earlier observation of melatonin-induced mitochondrial uncoupling.[45] These data further support that melatonin-induced uncoupling depends on complex II respiration, as melatonin-induced ROS production involved both complexes I and II. When complex II-linked substrates, such as succinate, are used, a portion of the electrons flows through complex I in the reverse direction. ROS produced under these conditions depend on the redox state of CoQ and $\Delta\psi m$.[16,32] Furthermore, our results showed that melatonin increased the $CoQ_{10}H_2/CoQ_{10}$ ratio and mitochondrial membrane potential (Figure 6). These results appear to be congruent with the finding that ROS production via

RET requires some essential mitochondrial features in the cell, such as the certain activity of mitochondrial complexes to maintain a high $\Delta\psi m$, especially the high activity of complex II to over-reduce the CoQ pool.[15] Furthermore, our data suggest that there is a correlation between the cell content of melatonin and ROS production, thus supporting the notion that high concentrations of melatonin in cancer cells are required to its the cytotoxic effect. Previously, we demonstrated that melatonin markedly decreases cell viability in the irradiated cells in a dose-dependent manner, especially at doses of 500 and 1500 μM. Surprisingly, 100 μM melatonin did not significantly reduce viability.[7] Consistently, other authors found that melatonin at high concentrations (10–1000 μM) was able to promote ROS generation and induced apoptosis in human leukemic Jurkat cells. When tested at concentrations of <10 μM, melatonin did not induce significant ROS generation in these cancer cells.[8]

Moreover, we recently demonstrated that high doses of melatonin, such as those used in this study and elsewhere,[46] significantly increased MT1 gene expression and led to a marked decrease in MT2 and RORα levels,[6] suggesting that melatonin receptor expression may be involved, at least partly, in the indoleamine effect.[31]
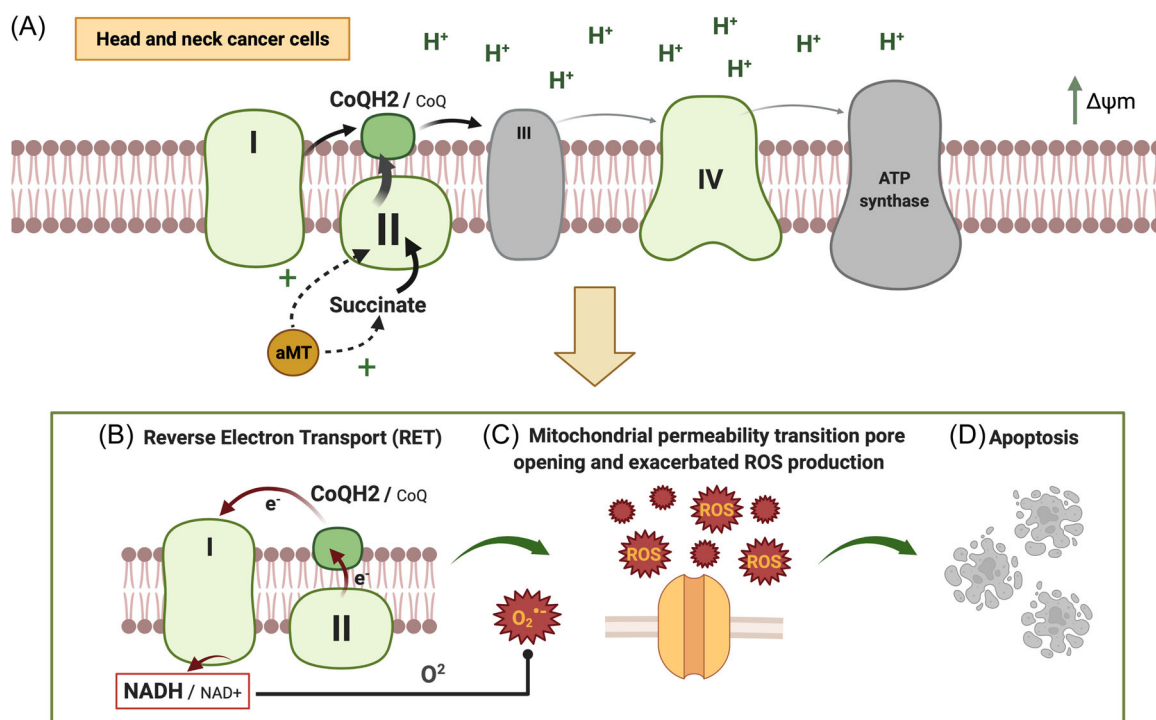

FIGURE 6 Melatonin mediates apoptosis in head and neck cancer by driving RET to induce ROS production. (A) Melatonin increases succinate levels, complex I, complex IV, and highly complex II activity and expression inducing an increase in CoQH$_2$/CoQ ratio and $\Delta\psi m$. (B) As a consequence, melatonin induces RET-ROS. (C), which leads to mitochondrial transition pore opening and exacerbated ROS production. (D) Finally, a high amount of ROS produces cancer cell apoptosis. Image created with BioRender.com. CoQ, coenzyme Q; RET, reverse electron transport; ROS, reactive oxygen species.

Finally, using AOX, a cyanide-insensitive oxidase that transfers electrons from QH_2 to oxygen and thus inhibits RET-ROS production, we confirmed the mechanism of action of melatonin in inducing ROS production in cancer cells via complex I RET. In vitro results in the current work demonstrated that complex I RET mediated the proapoptotic effects of melatonin via ROS production (Figure 6). Consistent with this finding, in vivo expression of AOX in a Cal-27 xenograft model abolished the therapeutic effects of melatonin

The question that arises is why melatonin produces large amounts of ROS by RET at complex I in HNSCC cells. In response to hypoxia, hypoxia-inducible factor (HIF) maintains ROS production at a physiologically low level and sustains integrity by decreasing respiratory activity.[47] However, melatonin can destabilize HIF-1α.[48] Previously, we have shown that melatonin inhibits tumor cells by reversing aerobic glycolysis.[6] Therefore, a key step in melatonin-based suppression of aerobic glycolysis is to destabilize HIF-1α.[49] These results align with the current observation that melatonin increased Krebs cycle intermediates, including succinate and respiratory capacity (Figure 6).

Our data show for the first time that melatonin induces ROS complex I RET under anaerobic metabolism and leads to apoptosis from excessive ROS production, only at high doses. This pathway likely represents a new mechanism underlying the oncostatic actions of melatonin in HNSCC cells.

AUTHOR CONTRIBUTIONS
Conceptualization: Germaine Escames. *Methodology*: Germaine Escames, Javier Florido, Laura Martinez-Ruiz, and César Rodriguez-Santana. *Formal analysis*: Germaine Escames, Javier Florido, and Laura Martinez-Ruiz. *Investigation*: Javier Florido, Laura Martinez-Ruiz, César Rodriguez-Santana, Alba López-Rodríguez, Agustín Hidalgo-Gutiérrez, Cécile Cottet-Rousselle, Frédéric Lamarche, Ana Guerra-Librero, Paula Aranda-Martínez, and Luis C. López. *Resources*: Germaine Escames and Uwe Schlattner. *Writing-original draft preparation*: Germaine Escames and Javier Florido. *Writing-review and editing*: Germaine Escames, Javier Florido, Uwe Schlattner, Darío Acuña-Castroviejo, and Luis C. López. *Supervision*: Germaine Escames, Uwe Schlattner, Darío Acuña-Castroviejo, and Luis C. López. *Project administration*: Germaine Escames. *Funding acquisition*: Germaine Escames

ACKNOWLEDGMENTS

CONFLICT OF INTEREST
The authors declare no conflict of interest.

DATA AVAILABILITY STATEMENT
The data that support the findings of this study are available from the corresponding author upon reasonable request.

ORCID
Darío Acuña-Castroviejo http://orcid.org/0000-0002-9680-1560
Germaine Escames http://orcid.org/0000-0003-1256-7656

REFERENCES
1. Mehrzadi S, Pourhanifeh MH, Mirzaei A, Moradian F, Hosseinzadeh A. An updated review of mechanistic potentials of melatonin against cancer: pivotal roles in angiogenesis, apoptosis, autophagy, endoplasmic reticulum stress and oxidative stress. *Cancer Cell Int.* 2021;21:1-28. doi:10.1186/s12935-021-01892-1
2. Pisani P, Airoldi M, Allais A, et al. Metastatic disease in head & neck oncology. *Acta Otorhinolaryngol Ital.* 2020;40:S1-S86. doi:10.14639/0392-100X-suppl.1-40-2020
3. Johnson DE, Burtness B, Leemans CR, Lui VWY, Bauman JE, Grandis JR. Head and neck squamous cell carcinoma. *Nat Rev Dis Prim.* 2020;6:92. doi:10.1038/s41572-020-00224-3
4. Hanna GJ, O'neill A, Shin K-Y, et al. Neoadjuvant and adjuvant nivolumab and lirilumab in patients with recurrent, resectable squamous cell carcinoma of the head and neck. *Clin Cancer Res.* 2021;28:468-478. doi:10.1158/1078-0432.ccr-21-2635
5. Shen YQ, Guerra-Librero A, Fernandez-Gil BI, et al. Combination of melatonin and rapamycin for head and neck cancer therapy: suppression of AKT/mTOR pathway activation, and activation of mitophagy and apoptosis via mitochondrial function regulation. *J Pineal Res.* 2018;64:1-18. doi:10.1111/jpi.12461
6. Guerra-Librero A, Fernandez-Gil BI, Florido J, et al. Melatonin targets metabolism in head and neck cancer cells by regulating mitochondrial structure and function. *Antioxidants.* 2021;10:1-20. doi:10.3390/antiox10040603
7. Fernandez-Gil BI, Guerra-Librero A, Shen YQ, et al. Melatonin enhances cisplatin and radiation cytotoxicity in head and neck squamous cell carcinoma by stimulating mitochondrial ROS generation, apoptosis, and autophagy. *Oxid Med Cell Longev.* 2019;2019:7187128. doi:10.1155/2019/7187128
8. Wölfler A, Caluba HC, Abuja PM, Dohr G, Schauenstein K, Liebmann PM. Prooxidant activity of melatonin promotes fas-

14 of 15 | WILEY—*Journal of Pineal Research*
Molecular, Biological, Physiological and
Clinical Aspects of Melatonin

FLORIDO ET AL.

induced cell death in human leukemic Jurkat cells. *FEBS Lett.* 2001;502:127-131. doi:10.1016/S0014-5793(01)02680-1

9. Moreira AJ, Ordoñez R, Cerski CT, et al. Melatonin activates endoplasmic reticulum stress and apoptosis in rats with diethylnitrosamine-induced hepatocarcinogenesis. *PLoS One.* 2015;10:e0144517. doi:10.1371/journal.pone.0144517

10. Tan DX, Manchester LC, Terron MP, Flores LJ, Reiter RJ. One molecule, many derivatives: a never-ending interaction of melatonin with reactive oxygen and nitrogen species. *J Pineal Res.* 2007;42:28-42. doi:10.1111/j.1600-079X.2006.00407.x

11. Zhang HM, Zhang Y. Melatonin: a well-documented antioxidant with conditional pro-oxidant actions. *J Pineal Res.* 2014;57:131-146. doi:10.1111/jpi.12162

12. Martín M, Macías M, Escames G, León J, Acuña-Castroviejo D. Melatonin but not vitamins C and E maintains glutathione homeostasis in t-butyl hydroperoxide-induced mitochondrial oxidative stress. *FASEB J.* 2000;14:1677-1679. doi:10.1096/fj.99-0865fje

13. Li Y, Li S, Zhou Y, et al. Melatonin for the prevention and treatment of cancer. *Oncotarget.* 2017;8:39896-39921. doi:10.18632/oncotarget.16379

14. Brand MD. The sites and topology of mitochondrial superoxide production. *Exp Gerontol.* 2010;45:466-472. doi:10.1016/j.exger.2010.01.003

15. Dröse S. Differential effects of complex II on mitochondrial ROS production and their relation to cardioprotective pre- and postconditioning. *Biochim Biophys Acta Bioenerg.* 2013;1827:578-587. doi:10.1016/j.bbabio.2013.01.004

16. Onukwufor JO, Berry BJ, Wojtovich AP. Physiologic implications of reactive oxygen species production by mitochondrial complex I reverse electron transport. *Antioxidants.* 2019;8:20-24. doi:10.3390/antiox8080285

17. Jia J, Wang Z, Zhang M, et al. SQR mediates therapeutic effects of H2S by targeting mitochondrial electron transport to induce mitochondrial uncoupling. *Sci Adv.* 2020;6:eaaz5752. doi:10.1126/sciadv.aaz5752

18. Scialò F, Fernández-Ayala DJ, Sanz A. Role of mitochondrial reverse electron transport in ROS signaling: potential roles in health and disease. *Front Physiol.* 2017;8:1-7. doi:10.3389/fphys.2017.00428

19. Fontaine E, Eriksson O, Ichas F, Bernardi P. Regulation of the permeability transition pore in skeletal muscle mitochondria modulation by electron flow through the respiratory chain complex I. *J Biol Chem.* 1998;273:12662-12668. doi:10.1074/jbc.273.20.12662

20. Fontaine E, Ichas F, Bernardi P. A ubiquinone-binding site regulates the mitochondrial permeability transition pore. *J Biol Chem.* 1998;273:25734-25740. doi:10.1074/jbc.273.40.25734

21. Vial G, Le Guen M, Lamarche F, et al. Liver mitochondrial function in ZDF rats during the early stages of diabetes disease. *Physiol Rep.* 2016;4:1-11. doi:10.14814/phy2.12686

22. Mao C, Liu X, Zhang Y, et al. DHODH-mediated ferroptosis defence is a targetable vulnerability in cancer. *Nature.* 2021;593:586-590. doi:10.1038/s41586-021-03539-7

23. González-García P, Hidalgo-Gutiérrez A, Mascaraque C, et al. Coenzyme Q10 modulates sulfide metabolism and links the mitochondrial respiratory chain to pathways associated to one carbon metabolism. *Hum Mol Genet.* 2020;29:3296-3311. doi:10.1093/hmg/ddaa214

24. Rao G, Murphy B, Dey A, et al. Cystathionine beta synthase regulates mitochondrial dynamics and function in endothelial cells. *FASEB J.* 2020;34(7):9372-9392. doi:10.1096/fj.202000173R

25. Monteiro L, de B, Davanzo GG, de Aguiar CF, Moraes-Vieira PMM. Using flow cytometry for mitochondrial assays. *MethodsX.* 2020;7:100938. doi:10.1016/j.mex.2020.100938

26. Al Kadhi O, Melchini A, Mithen R, Saha S. Development of a LC-MS/MS method for the simultaneous detection of tricarboxylic acid cycle intermediates in a range of biological matrices. *J Anal Methods Chem.* 2017;2017:1-12. doi:10.1155/2017/5391832

27. Hidalgo-Gutiérrez A, Barriocanal-Casado E, Bakkali M, et al. β- RA reduces DMQ/CoQ ratio and rescues the encephalopathic phenotype in Coq9 R239X mice. *EMBO Mol Med.* 2019;11:1-18. doi:10.15252/emmm.201809466

28. Chouchani ET, Pell VR, Gaude E, et al. Ischaemic accumulation of succinate controls reperfusion injury through mitochondrial ROS. *Nature.* 2014;515:431-435. doi:10.1038/nature13909

29. Acuña-Castroviejo D, Martín M, Macías M, et al. Melatonin, mitochondria, and cellular bioenergetics. *J Pineal Res.* 2001;30:65-74. doi:10.1034/j.1600-079X.2001.300201.x

30. López A, Ortiz F, Doerrier C, et al. Mitochondrial impairment and melatonin protection in parkinsonian mice do not depend of inducible or neuronal nitric oxide synthases. *PLoS One.* 2017;12:1-22. doi:10.1371/journal.pone.0183090

31. Ortiz F, Acuña-Castroviejo D, Doerrier C, et al. Melatonin blunts the mitochondrial/NLRP3 connection and protects against radiation-induced oral mucositis. *J Pineal Res.* 2015;58:34-49. doi:10.1111/jpi.12191

32. Murphy MP. How mitochondria produce reactive oxygen species. *Biochem J.* 2009;417:1-13. doi:10.1042/BJ20081386

33. Robb EL, Hall AR, Prime TA, et al. Control of mitochondrial superoxide production by reverse electron transport at complex I. *J Biol Chem.* 2018;293:9869-9879. doi:10.1002/ajmg.1398

34. Cadenas S. Mitochondrial uncoupling, ROS generation and cardioprotection. *Biochim Biophys Acta Bioenerg.* 2018;1859:940-950. doi:10.1016/j.bbabio.2018.05.019

35. Guarás A, Perales-Clemente E, Calvo E, et al. The CoQH2/CoQ ratio serves as a sensor of respiratory chain efficiency. *Cell Rep.* 2016;15:197-209. doi:10.1016/j.celrep.2016.03.009

36. Hidalgo-Gutiérrez A, Barriocanal-Casado E, Díaz-Casado ME, et al. β-RA targets mitochondrial metabolism and adipogenesis, leading to therapeutic benefits against CoQ deficiency and age-related overweight. *Biomedicines.* 2021;9(10):1457. doi:10.3390/biomedicines9101457

37. Sun TC, Liu XC, Yang SH, et al. Melatonin inhibits oxidative stress and apoptosis in cryopreserved ovarian tissues via Nrf2/HO-1 signaling pathway. *Front Mol Biosci.* 2020;7:1-11. doi:10.3389/fmolb.2020.00163

38. Wallace DC. Mitochondria and cancer Douglas. *Nat Rev, Cancer.* 2012;12:685-698. doi:10.1038/nrc3365.Mitochondria

39. Xu Y, Xue D, Bankhead A, Neamati N. Why all the fuss about oxidative phosphorylation (OXPHOS). *J Med Chem.* 2020;63:14276-14307. doi:10.1021/acs.jmedchem.0c01013

40. Szatrowski TP, Nathan CF. Production of large amounts of hydrogen peroxide by human tumor cells. *Cancer Res.* 1991;51:794-798.

41. Sabharwal SS, Schumacker PT. Mitochondrial ROS in cancer: initiators, amplifiers or an Achilles' heel. *Nat Rev Cancer.* 2014;14:709-721. doi:10.1038/nrc3803

42. Nogueira V, Park Y, Chen C-C, et al. Akt determines replicative senescence and oxidative or oncogenic premature senescence and sensitizes cells to oxidative apoptosis. *Cancer Cell.* 2008;14:458-470. doi:10.1016/j.ccr.2008.11.003

43. Zorov DB, Juhaszova M, Sollott SJ. Mitochondrial reactive oxygen species (ROS) and ROS-induced ROS release. *Physiol Rev.* 2014;94:909-950. doi:10.1152/physrev.00026.2013

44. Lambert AJ, Brand MD. Inhibitors of the quinone-binding site allow rapid superoxide production from mitochondrial NADH:ubiquinone oxidoreductase (complex I). *J Biol Chem.* 2004;279:39414-39420. doi:10.1074/jbc.M406576200

45. Bilska B, Schedel F, Piotrowska A, et al. Mitochondrial function is controlled by melatonin and its metabolites in vitro in human melanoma cells. *J Pineal Res.* 2021;70(3):1-19. doi:10.1111/jpi.12728

46. Venegas C, García JA, Doerrier C, et al. Analysis of the daily changes of melatonin receptors in the rat liver. *J Pineal Res.* 2013;54:313-321. doi:10.1111/jpi.12019

47. Fuhrmann DC, Brüne B. Mitochondrial composition and function under the control of hypoxia. *Redox Biol.* 2017;12:208-215. doi:10.1016/j.redox.2017.02.012

48. Yang L, Zheng J, Xu R, et al. Melatonin suppresses hypoxia-induced migration of HUVECs via inhibition of ERK/Rac1 activation. *Int J Mol Sci.* 2014;15:14102-14121. doi:10.3390/ijms150814102

49. He M, Zhou C, Lu Y, et al. Melatonin antagonizes nickel-induced aerobic glycolysis by blocking ROS-mediated HIF-1α/miR210/ISCU axis activation. *Oxid Med Cell Longev.* 2020;2020:1-14. doi:10.1155/2020/5406284

SUPPORTING INFORMATION

Additional supporting information can be found online in the Supporting Information section at the end of this article.